Chapter 5

Nanostructured Pure and Doped Zirconia: Syntheses and Sintering for SOFC and Optical Applications

Mythili Prakasam, Sorina Valsan, Yiying Lu, Felix Balima, Wenzhong Lu, Radu Piticescu and Alain Largeteau

Additional information is available at the end of the chapter

http://dx.doi.org/10.5772/intechopen.81323

Abstract

Zirconia is a multifunctional material with potential applications in wide domains. Rare-earth doped zirconia and stabilized zirconia yield interesting properties based on the phase transitions induced by the sintering conditions. Zirconia nanopowders were prepared by hydrothermal technique. Synthesis methods of zirconia with various rare earths are discussed here. An overview of the sintering of zirconia-based ceramics is presented in particular for SOFC and sensors and optical applications.

Keywords: sintering, solid oxide fuel cell, optical ceramics, hydrothermal syntheses

1. Introduction

Zirconia (ZrO_2) is one of the materials well known for multifunctional applications [1–8]. Commonly employed application domains of ZrO_2 are refractories [9], oxygen sensors [10], and fuel cell membranes [11] due to the high O_2 diffusivity, structural [12], and biomedical applications [13] due to its high strength and toughness. ZrO_2 with its higher birefringence than alumina [14] makes it to be employed in miniature optical devices. Two crystallographic transformations are experienced by ZrO_2 between room temperature and its melting point (~2715°C) such as monoclinic to tetragonal [15] at ~1170°C and tetragonal to cubic [16] at ~2370°C. The high temperature tetragonal and cubic forms are stabilized with different elements, such as Mg, Ca, Sc, Ce, and Y [17]. Existence of Cubic ZrO_2 until room temperature, which is named FSZ (fully stabilized zirconia), can be observed with concentration of 8% Yttria [18]. Stabilized

zirconia in particular with Yttria called YSZ is widely used for a variety of applications such as thermal barrier material, and with additional optical characteristics such as transparency/translucency, they are used as windows [19] for anvil cells, infrared windows, laser host materials, armor applications, optical lenses, tooth-like esthetics, thermal insulating transparent windows, scratch-resistant electronics, bar scanners and high pressure sodium, and mercury halide lamps. Initially, YSZ single crystals [20] were widely known for its use as artificial gemstones and high thermal shock behavior. Nevertheless, owing to the advantages [21] of polycrystalline transparent ceramics in terms of time, cost, size, shape, and mechanical strength have recently been studied to replace single crystals. Due to the inherent birefringence, additional light scattering will be experienced in addition to the grain boundaries. In this chapter, we have focused our attention on the application of ZrO_2 for SOFC and optical transparent ceramics. Syntheses of rare earth doped ZrO_2 nanopowders by hydrothermal method are discussed.

2. Zirconia phases

The phase diagram of zirconia is very well known in the literature. The polymorphism of zirconia is presented in the scheme (**Figure 1**) below:

The different phases of pure zirconia are clearly identified in **Figure 2**. Indeed, without stabilization with yttria, zirconia is present in monoclinic form until a temperature of 1170°C, where it leaves room for the tetragonal phase. The cubic phase, meanwhile, can be obtained only from a temperature of 2370°C.

It is also noted that stabilization with yttria at 3 and 8% facilitates the organization of the zirconia crystals in the tetragonal phase, which is close to the cubic phase while avoiding the unstable monoclinic phase. The concentration of phase is stabilized partially with 3% of Y_2O_3, usually called partially stabilized zirconia (PSZ) (3YSZ), where both the monoclinic and tetragonal phases coexist. When the concentration of Y_2O_3 reaches 8%, all the monoclinic phases are converted into tetragonal called as fully stabilized zirconia (FSZ) (8YSZ). Cubic phase is obtained with increasing Y_2O_3 concentration, and the temperature required for densification is too high. It is known that the crystalline phase is easier to achieve than conventional crystal structures, but it is not possible to transform the phase into a monoclonal phase in the case of pure ZrO_2. It follows therefore that the more the zirconia is stabilized and the more it will be possible to obtain a phase that will have the desired optical properties.

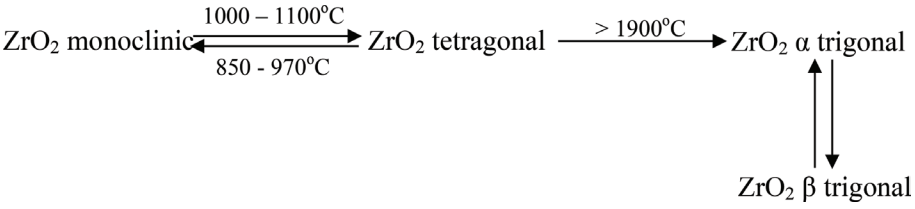

Figure 1. Different crystalline phases of zirconia with respect to temperature.

http://dx.doi.org/10.5772/intechopen.81323

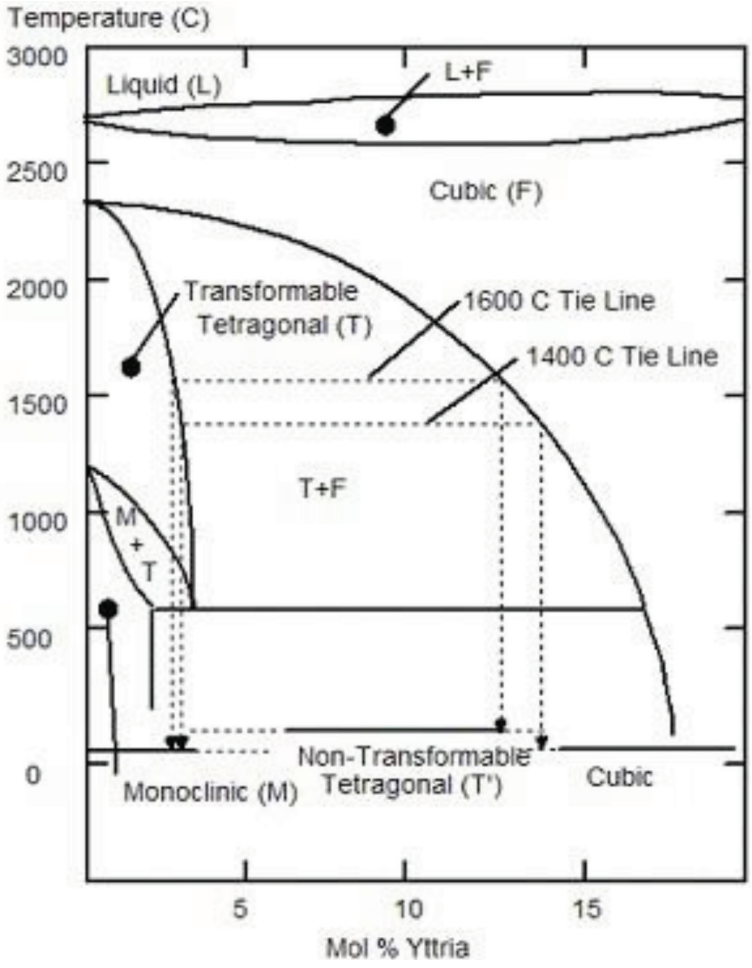

Figure 2. Phase diagram of zirconia with yttria stabilization.

The transition from tetragonal to monoclinic phase is done with a volume increase of about 4% leading to microcracking that drastically affects the mechanical properties. Therefore, the stabilization of cubic or tetragonal phase on larger temperature ranges is required for safety application. The tetragonal or cubic phase can be stabilized (e.g., the temperature of the "$c \rightarrow t$" transition may be decreased) by inducing such additives as MgO, CaO, Y_2O_3, and other rare earth oxides, etc. The doping elements affect not only the structural and mechanical properties but also optical and electrical behavior. Synthetically, the binary system of ZrO_2 may be classified into different systems as specified by Haberko et al. [22]: systems forming cubic solid solutions in the rich ZrO_2 domain: ZrO_2–MeO (Me = Mg, Cr, Co, Cu), ZrO_2–Me_2O_3 (Me = Fe, Cr, La,), ZrO_2–Me_3O_4 (Me = Fe, Mn), ZrO_2–MeO_2 (Me = Th, Ce); systems with the formation of other types of solid solutions in the rich ZrO_2 domain: HfO_2–ZrO_2, TiO_2–ZrO_2, etc.; and

systems with no interactions between the components, e.g., ZnO–ZrO_2, Al_2O_3–ZrO_2. Zirconia ceramic materials are known as important candidates for functional and structural applications. Stabilized Y_2O_3–ZrO_2 ceramics (YSZ) is the most common solid electrolyte used in various applications as oxygen sensors or fuel cells in automotive industry, metallurgical, glass and cement industries, gas pumps for removing oxygen traces from the gases used in special industrial processes, and fuel cells. Their utilization opened a new way for optimization of oxygen (air)/fuel ratios and made automotive and industries more environment friendly due to its adequate level of oxygen ion conductivity and desirable stability in both oxidizing and reducing atmospheres [23]. In principle, these sensors use the Nernst voltage generated by the difference of two different ion concentrations (with different partial pressures) on the sides of an electrolyte, which generate an electrical potential. This voltage is proportional to the natural logarithm of the ratio of the two different ion concentrations according to the Nernst equation:

$$\Delta U = \frac{k_B T}{e_0} = \ln \frac{c_1}{c_2} \tag{1}$$

where k_B is the Boltzmann constant (= 1.38×10^{-23} J/K), T is the absolute temperature in K, e_0 is the elementary charge (1.602×10^{-19} C), and c_i is the ion concentration on the two sides of the solid electrolyte in mol/kg. The mechanism of zirconia partial oxygen pressure sensors is basically described below. At temperatures higher than a certain activation value depending on the composition and structure, zirconia partly dissociates to produce oxygen ions, which can be transported through the material when a voltage is applied. Due to this process, zirconia behaves like a solid electrolyte for oxygen. If two different oxygen pressures exist on either side of a zirconia material, the Nernst voltage can be measured across that element. Generally, ZrO_2-8 mol%Y_2O_3 (YSZ) solid electrolytes exhibiting a conductivity of about 0.1 Ω^{-1} cm^{-1} at 1000°C and about 3×10^{-5} Ω^{-1} cm^{-1} at 400°C corresponding to an activation energy of 96 kJ mol^{-1} are used.

2.1. Rare earth doped zirconia phases

To improve the ionic conductivity and sensors' quality factors in a large temperature range, different approaches were proposed: partial or total replacement of Y_2O_3 with Sc_2O_3 having a maximum corresponding to the composition $(Y_{0.5}Sc_{0.5})$*0.3 $Zr_{0.7}O_{1.85}$. The main limitation of this approach is the decrease of conductivity observed with holding time due to the structural modifications [24]**.** The development of planar sensors using ceramic membranes and multipackaging technology in place of classical bulk sintered materials shows the ability to increase the efficiency of the thermal transfer but has limited effect on the ionic conductivity of the material itself [25]**.** In this case, the technology is the main limiting factor, since complex additives are required to control the dispersibility of the ceramic powders [26]. Reducing the diffusion and transport distances using nanocrystalline membranes and thin films, Kosacki et al. found that nanocrystalline YSZ thin films with mean grain sizes in the range 10–200 nm materials exhibited two-three orders of magnitude increase in conductivity compared to polycrystalline and single crystalline materials [27]. An activation energy in the range 0.85 ± 0.05 eV for bulk conductivity with a corresponding grain boundary conductivity of 1.0 ± 0.1 e for nanocrystalline 2–3 mol% Y_2O_3 doped ZrO_2 ceramics with average grain particle in the range 35–50 nm was reported. It was also reported that yttria doped tetragonal

zirconia (YTZP) ceramics have lower activation energy for the ion conduction opening the field for their utilization at lower temperatures [28]. A comprehensive review with respect to the structure, chemistry, design and selection of materials, underlying mechanisms, and performance of each SOFC component, which opens up the future directions toward pursuing SOFC research, was recently proposed in [29].

Zirconia co-doped with different rare earth elements has been intensively studied during recent period due to the versatility of these materials in various optoelectronic devices and biomaterials. Some examples are summarized below. A single step, rapid microwave driven solution combustion technique was used to obtain luminescent, cubic ZrO_2: Eu^{3+}nanophosphors [30]. Zirconia doped with selected trivalent rare earth oxides was successfully obtained by a complex polymerization method and may be considered promising candidates for white light-emitting applications [31]. ZrO_2:Eu^{3+} nanocrystals were synthesized by hydrothermal technique. Effects of Eu^{3+} doping and annealing on the morphology, crystal structure, and fluorescence properties of the resultant nanocrystals were investigated. Nanocrystals with tetragonal or cubic structure may find potential applications as the raw material for producing the transparent ceramics with efficient fluorescence properties [32]. Zirconium oxide powders doped with terbium, synthesized by hydrothermal route from a highly basic solution, were used to determine the role of the basic agent (NaOH, KOH, or LiOH) utilized to carry out the hydrothermal synthesis on their morphology, crystalline structure, photoluminescent, or cathodoluminescent properties [33]. Scandia-stabilized zirconia powder (ScSZ) was synthesized by a microwave-hydrothermal method. The structure of the ScSZ powder changed from a tetragonal to a cubic phase, and accordingly, the powder conductivity was increased from 90.55 to 120.56 mS/cm by the introduction of the mineralizer solutions (KOH + K_2CO_3) during the microwave-hydrothermal processing [34]. Un-doped and rare earth (Dy and Ce)-doped ZrO_2 nanoparticles NPs were synthesized by coprecipitation method, showing no toxicity and possessing good antibacterial ability [35]. The thermal stability of zirconia up to very high temperatures explains also its intensive use in energy generation applications as coatings or sintered bulk pieces. Thermal barrier coatings (TBCs) have proved to be a key technology in thermal stability, and their use to achieve surface temperature reduction of the underlying super alloys surpass all other achievements in the field of material technologies that have taken place in last three decades [36].

2.2. Zirconia nanopowder syntheses

The technique most often used to prepare zirconia powders is the sol-gel route. The sol-gel process makes it possible to manufacture an inorganic polymer by simple chemical reactions and at a temperature close to room temperature. The synthesis is carried out from precursors. They are either liquid or solid and are mostly soluble in common solvents. The simple chemical reactions at the base of the process are triggered when the precursors are brought into contact with water. To prepare the pure zirconia powders [37–41], the precursor used is zirconium n-propoxide ($Zr(OC_3H_7)_4$, 70% diluted in n-PrOH) [42]. Sol-gel synthesis can also be carried out to obtain zirconia powders doped with 3% of Yttria [43].

Another technique used in the synthesis is coprecipitation [44]. It is a simultaneous precipitation of two substances, and it is used for the preparation of 8YSZ. To do this, we must precipitate Zr^{4+} and Y^{3+}. The synthesis of the powders can also be obtained by pyrolysis of spray

aerosol (spray-pyrolisis). This process involves injecting the spray containing the precursor solution into a combustion chamber where the particles are quickly ignited. This technique makes it possible to obtain zirconia powders doped with Yttria [45] and in particular doped with 8YSZ [46]. It is also possible to use a hydrothermal route to synthesize zirconia powders [47]. Hydrothermal synthesis allows the production of crystalline fine powders to deagglomerate. These qualities are suitable for the preparation of fine oxide/oxide composites by simultaneous synthesis of the two phases. The last technique that can be used is a homogeneous precipitation method of zirconium oxychloride, yttrium, urea, which is used as a precipitating agent, and polyacrylic acid, which is used as a dispersing agent [48].

2.2.1. Synthesis methods for RE doped ZrO_2, with accent on hydrothermal synthesis

The so-called triangle synthesis, properties, and applications must be fully exploited to obtain assessed materials for specific applications. The properties of nanostructured materials depend on the atomic structure, composition, microstructure, defects, and interfaces, which are controlled by thermodynamics and kinetics of the synthesis. Different synthesis routes for manufacturing of nanomaterials were proposed. Generally, they may be classified as physical, chemical, and combined routes. Other classification considers the top-down approach from the macroscale to the nanoscale or conversely by assembly of atoms or particles using the bottom-up approach. Chemical reactions for material synthesis can be done in solid (conventional synthesis route), liquid, or gaseous state. For solid state reactions, diffusion of atoms depends on the temperature of the reaction, and transport across grain boundaries and grain growth at elevated temperature reactions may lead to solids with large grain size. Compared to solid-state synthesis, diffusion in the liquid or gas phase is typically and advantageously many orders of magnitude larger than in the solid phase; thus, the synthesis of nanostructured materials can be achieved at lower temperatures, reducing the detrimental grain growth.

Synthesis route	**Solid-state process**	**Coprecipitation**	**Hydrothermal**	**Sol-gel**	**Spray pyrolysis**
Composition control	Poor	Good	Excellent	Medium	Excellent
Morphology control	Poor	Medium	Good	Medium	Good
Particle size (nm)	>1000	>100	10–100	>10	>10
Hard agglomerates	Medium	High	Low	Medium	Low
Impurities (%)	0.5–1	Max. 0.5	Max. 0.5	0.1–0.5	0.1–0.5
Additional steps	Calcinations, milling	Calcinations, milling	No	Calcinations, milling	No
Scalability	Industrial	Industrial	Demonstration	Demonstration	R&D
Environmental impact	High	Moderate	Low	High	Moderate

Table 1. A comparison between main synthesis routes for obtaining doped zirconia materials.

Although many laboratory-scale reactions can be scaled up to economically produce large quantities of materials, the laboratory-scale reaction parameters may not be linearly related to that of large-scale reaction. The synthesis parameters such as temperature, pH, reactant concentration, and time should be ideally correlated with factors such as supersaturation, nucleation and growth rates, surface energy, and diffusion coefficients in order to ensure the reproducibility of reactions. A comparison between the main procedures used for the synthesis of doped zirconia materials is presented in **Table 1** from the point of view of scalability.

The main advantages of the hydrothermal synthesis are one step process for powder synthesis or oriented ceramic films; minimized consumption energy; closed-flow system; relatively high deposition rate; products with much higher homogeneity than solid state processing; products with higher density than gas or vacuum processing (faster growth rate); and versatility: oxides, nonoxides, organic/biologic materials, and hybrid materials with different morphologies may be obtained [49].

3. Classical sintering of rare earth doped zirconia

Different theoretical and empirical models for solid state sintering were used for modeling the density of sintered zirconia nanomaterials using classical pressing and sintering technology, however being limited by the complexity of the structural modifications during the compaction process. A study on the influence of the synthesis and processing parameters on the ion conduction of YTZP nanomaterials and the characteristics of gauges for pressure sensors was performed [50]. YTZP powders (ZrO_2 doped with 3.5 mol% Y_2O_3) obtained by hydrothermal treatment of the precursor suspensions in a Teflon autoclave for various times at temperatures around 250°C using ammonia as mineralizing agent were used in the sintering studies.

Powders with very high specific surface area (195–200 m^2/g) and pycnometric density in the range 5–5.2 g/cm^3 were used. YTZP powders obtained via the hydrothermal procedure having the microstructure and properties described before were used (**Figure 3**) to obtain compact materials via two methods:

- Bulk material by pseudo-axial pressing and sintering.
- Tape casting of membranes followed by drying and sintering.

The sintered bulk material was obtained by pseudo-biaxial pressing at 100 MPa followed by sintering in air. To eliminate the chemically bonded water, powders have been additionally attrition milled for 2 hours in acetone before addition of sintering additives. The optimal sintering parameters were estimated from the dynamic sintering curves obtained by the heating stage microscopy (**Figure 4**). Two shrinkage intervals can be clearly observed, the first from room temperature to approximately 550°C related to thermal decomposition of binders (polyvinyl alcohol PVA) and the second at 1400°C corresponding to sintering, with a total shrinkage of 28% at 1400°C. Compacts with densities higher than 96% of the theoretical and grain sizes around 200 nm have been obtained.

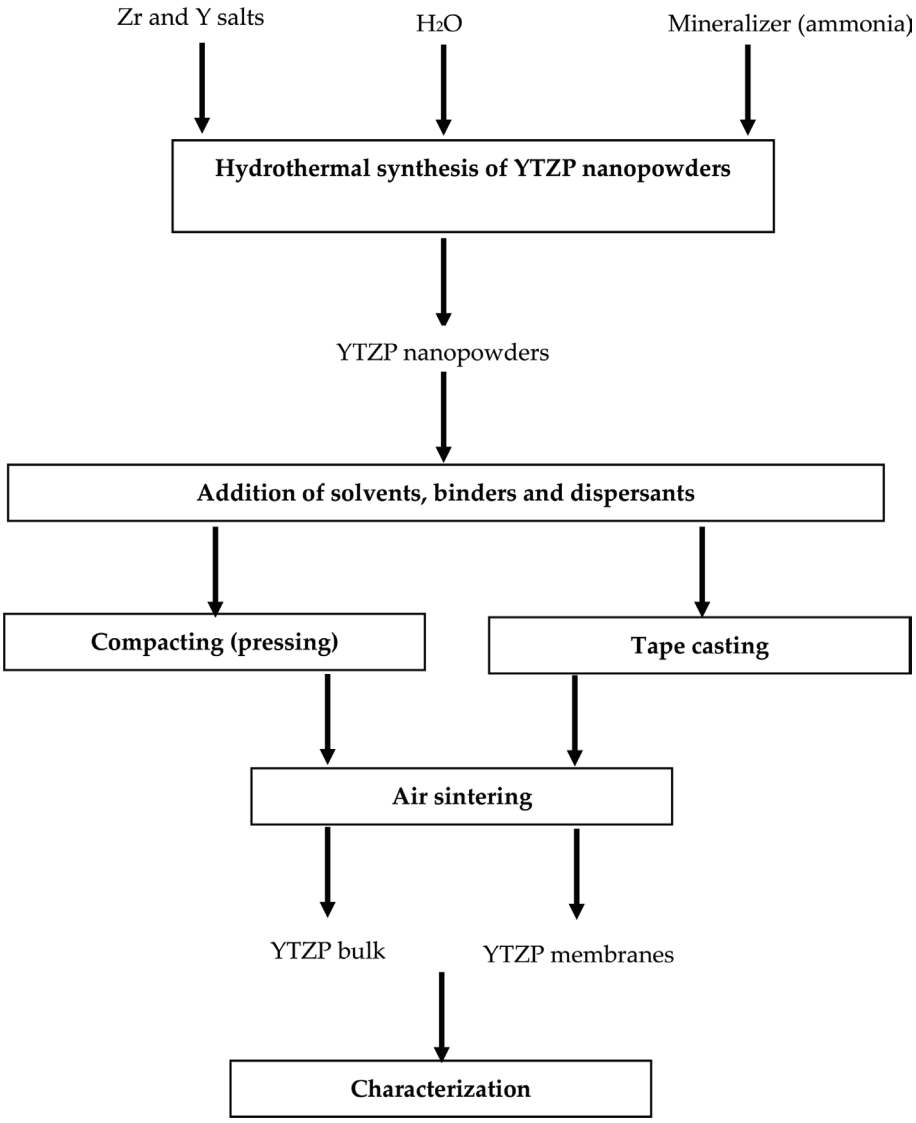

Figure 3. Schematic flow sheet for obtaining of YTZP materials for sensors application.

The effective ionic conductivity of YTZP bulk materials was measured using impedancemetry measurements**.** The contributions of bulk and grain boundaries on the total ionic conductivity were calculated from the impedance spectra of samples. The results on the activation energy of ionic conduction are presented in **Table 2** below.

The model developed suggest that grain boundaries increase the total ionic conductivity of yttria-doped zirconia due to a "short circuit effect," leading to an apparent conductivity

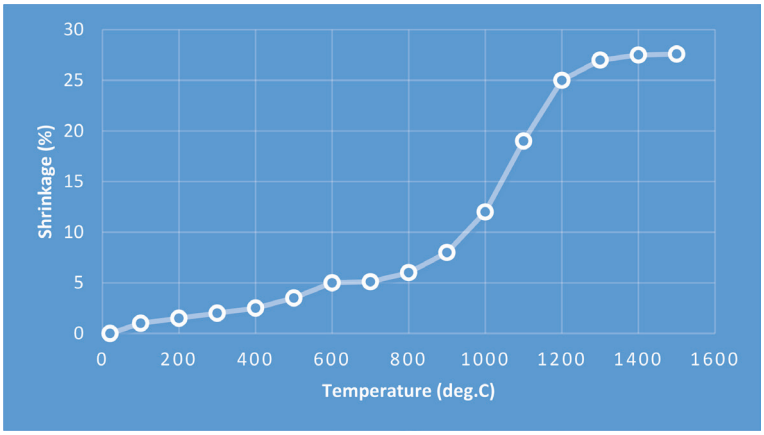

Figure 4. Dynamic sintering curves of YTZP nanopowders.

Y_2O_3 mol% in YTZP	Grain sizes (nm)	Microstructure	Activation energy of ionic conductivity (kJ/mol)
7.5	625	Polycrystalline	110
3	524	Polycrystalline	97.5
3	393	Polycrystalline (0.25% Al_2O_3 (grain growth inhibitor))	86
4	603	Polycrystalline	90
3		Single crystal	84

Table 2. Activation energy of ionic conductivity in YTZP nanomaterials.

higher than of single crystals of similar composition. This effect increases with decreasing grain sizes and may practically neglect large micrometric grain sizes.

3.1. New sintering methods of rare earth doped zirconia

Various sintering techniques [51] have been employed till date for the fabrication of YSZ transparent ceramics. Most prevalently used techniques are hot isostatic pressing [52], spark plasma sintering (SPS) [53], and microwave sintering [54]. Different approaches have been employed for obtaining transparent ceramics [55] of YSZ either by means of dopant, high pressure, two-step load application procedure, or pre compaction followed by vacuum sintering and hot isostatic pressing. Kim et al. [56] studied the effects of the sintering conditions of dental zirconia ceramics on the grain size and translucency by comparing the microwave sintering and classical sintering. Jiang et al. [57] analyzed the effects of sintering temperature and particle size (40 and 90 nm) on the 3YSZ (YSZ with 3% Y_2O_3) dental ceramic because 3% Y_2O_3 gives higher mechanical strength than 8% Y_2O_3. Fang et al. [58] showed enhanced densification of zirconia containing ceramic matrix composites by microwave processing. Tamburini

et al. [59] reported on high pressure SPS, whereas Casolco et al. [60] used a traditional die set-up and two-step load application procedure. Klimke et al. and Krell et al. [14, 61] used CIP followed by HIP, whereas Tosoh [62] Corporation and their team used sintering aid such as TiO_2 to obtain transparent 8YSZ (YSZ with 8% Y_2O_3). The addition of TiO_2 is reported to decrease the mechanical strength [63] of 8YSZ transparent ceramics with low transparency.

Zirconia powders doped with 3 mol% Y_2O_3 and co-doped with 3 mol% Y_2O_3–6 mol% CeO_2 have been selected for preliminary sintering tests using a field assisted method [64]. The hydrothermally synthesized powders after were mixed with a solution containing 6 wt% polyvinyl alcohol as binder and spray dried using a LabPlant spray drier system (air speed of 3.5 m/s at evacuation and feeding rate of 617 ml/h using a 0.5 mm nozzle). Rapid analysis by optical micrographs of all investigated samples revealed the presence of rounded particles with sizes ranging from a few microns to tens of microns. The powder morphology was maintained after the heat treatment for 2 hours at 500°C to remove the PVA binder, and they have been further used in FAST sintering tests, using a thermal mechanical simulator—Gleeble 3800, with fully integrated digital closed-loop control thermal and mechanical testing system makes highly accurate process control possible. The tests were conducted with variation of different key parameters, such as pressure, maximum temperature, and holding time, where the temperature range applied was 1100–1300°C, with pressure range of 75–125 MPa and holding time of 120–240 second.

The relative density of the sample was calculated to 99.47%, which was under the sintering condition at 1300°C and 125 MPa, with 25°C/S heat rate and 120 Sholding time. It may be observed that no open porosity exists, which indicates that a fully dense bulk material was achieved (**Figure 5**).

Flash sintering is also a new sintering method that attracted significant attention for rapid densification of ceramics at low sintering temperatures, allowing to retain the fine grains and control the dielectric and mechanical properties. Flash sintering of yttria-stabilized zirconia at temperatures <600°C with a constant heating rate of 25°C/min leads to dense ceramics

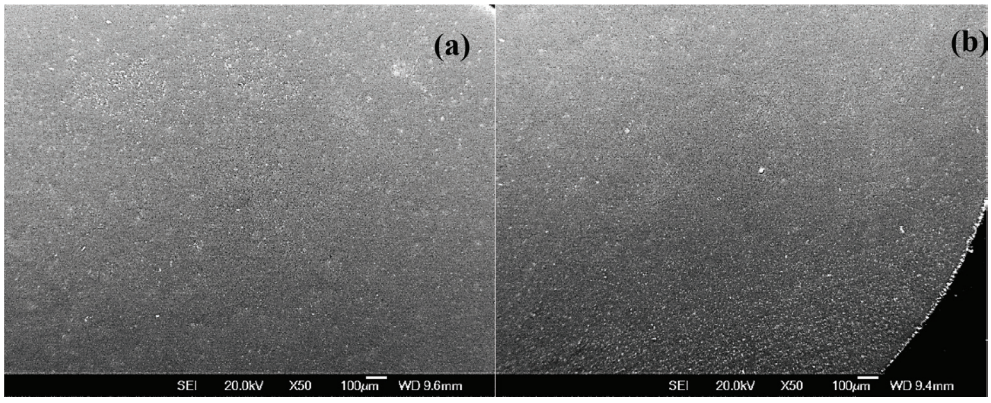

Figure 5. SEM micrographs of sintered samples (a) ZrO_2-3Y and (b) co-doped with 3Y-6CeO_2-ZrO_2.

with high ultimate compressive strength >3.5 GPa and inelastic strain around 8% due to the transformation toughening. At higher temperatures, the high dislocation density induced by the flash sintering conditions improves the plasticity of the sintered ceramics and retards the cracks nucleation and propagation [65].

3.2. Classification of transparent materials and applications of transparent ceramics

Nowadays, materials such as glasses, polymers, or single crystals are used for applications requiring good optical properties such as laser, lenses, camera domes, and much more.

However, transparent ceramics are an interesting alternative to the aforesaid materials. Indeed, they have a greater ease of development of large complex parts, good mechanical properties (good resistance to thermal shocks and fractures), low thermal expansion, good thermal conductivity, and good tenacity. They are already used for various applications.

3.2.1. The manufacture of transparent ceramics

Transparent ceramics can be classified into two different forms based on their crystalline structure: the cubic structure and the noncubic structure. The cubic transparent ceramics is one of the widely reported in the literature. Manufacture of noncubic transparent ceramics is not an easy task, which can be explained as below. Depending on the type of structure, there will be the problem of birefringence occuring at the grain boundaries. For the noncubic structure, the material is said to be anisotropic. In this case, we observe two indices of refraction: the ordinary index and the extraordinary index. This extraordinary ray is going to make our material birefringent, and it will be necessary to control very closely the growth of the grains, due to the diffusion of light caused by the ceramics with birefringence.

The methods of fabrication of transparent ceramics are numerous such as hot pressing, hot isostatic pressing, vacuum sintering, microwave sintering, and spark plasma sintering.

3.2.2. Rare earth-based zirconia-based transparent ceramics by spark plasma sintering

Until to date, there are no reports focusing on yielding 3YSZ and 8YSZ transparent ceramics by analyzing sintering parameters and their influence in yielding transparency by SPS sintering. Here, we report on yielding 3YSZ transparent ceramics containing tetragonal phases without addition of any dopants or high-pressure technique. Tetragonal phased zirconia has interesting mechanical strength due to its large refractive index and high dielectric constants. In order to obtain transparent ceramics, it is necessary to have maximum density and minimum porosity in the orders of <0.01 vol% in the final sintered body. The aforesaid is achieved due to the interplay of various sintering parameters (SP) such as sintering temperature, dwell time, heating/cooling rate, pressure, and temperature of pressure application. We have optimized the sintering parameters and demonstrated the possibility of obtaining transparent 3YSZ through reactive sintering during spark plasma sintering favorizing cubic phase formation with Y segregation around the grain boundaries. We demonstrated for the first time the presence of tetragonal and cubic phases in transparent ceramics of 3YSZ and 8YSZ obtained by SPS. The experimental details and results are presented in the following sections.

In the present study, 3YSZ and 8YSZ nanopowders (Tosoh Corporation) with average crystallite size ~20 nm average particle diameter 0.3 μm were used for the fabrication of 3YSZ and 8YSZ transparent ceramics. Spark plasma sintering (SPS) experiments were performed with DR. SINTER LAB Spark Plasma Sintering system, Model SPS-515S-FUJI. The experiments were performed under a vacuum of 10 Pa with the pulse sequence for the SPS applied voltage of 12:2 (i.e., 12 ON/2 OFF). 1 g of powder was used for each experiment. The experiment was carried out in a graphite mold with inner diameter of 10 mm and external diameter of 25 mm. The internal of the graphite die was covered with carbon foil (Papyex). The mold was covered with carbon fiber felt to limit the loss of heat radiation. Due to the usage of pyrometer, the temperature was first increased to 600°C within 3 min without regulation and then increased to a range of temperatures from 1150–1400°C with different heating rate (R_H) ranging from 2.5 to 100°C/min and with 20 min dwell time. Uniaxial pressures ranging from 40 to 100 MPa were applied at room temperature (T_R) and sintering temperature (T_S), and their significances have been analyzed. The cooling rates (R_C) and R_H were maintained equal in all the experiments. Then, the ceramics were ground and polished to a thickness of 1 mm with optical finishing. Powder X-ray diffraction (XRD) analysis was performed with a PANalytical X'Pert MDP diffractometer with θ-θ Bragg Brentano configuration, with a backscattering graphite monochromator for K_α Cu radiation working at 40 kV and 40 mA. Temperature dependent XRD has been performed using a powder diffractometer (PANalytical X'Pert Pro) equipped with a high-temperature chamber Anton Paar HTK16 (1600° C) measuring with K_α Cu radiation. The temperatures of analyses used were from room temperature until 1400°C. The density was measured by the Archimedes method in distilled water. The microstructure was observed by a scanning electron microscope (Joel 840 SEM) on fractured surface without polishing. The optical transmittance spectrum was measured by using a double beam spectrophotometer (Varian Cary 5000) at a range of between 200 and 7000 nm for a sample thickness of 1.5 mm.

It has to be mentioned that so far the ceramics of pure monoclinic ZrO_2 did not yield transparency, whereas the samples of 3YSZ were translucent and that of 8YSZ are well transparent. In order to study the behavior of ZrO_2 with three different compositions, all the samples were treated under same conditions, i.e., sintering temperature = 1200°C, heating/cooling rate = 2.5°, 5°, and 10°C/min, dwell time = 20 min, pressure applied = 100 MPa, and point of pressure application at the start of sintering cycle and the other being only during the dwell time. Though transparency was obtained for the pure ZrO_2, the sample was dense under the following conditions: sintering temperature = 1200°C, heating/cooling rate = 2.5°C/min, dwell time = 20 min, pressure applied = 100 MPa, and point of pressure application = only during the dwell time. The translucent sample of 3YSZ was obtained at sintering temperature = 1200° C, heating/cooling rate = 2.5°C/min, dwell time = 20 min, pressure applied = 100 MPa, and point of pressure application = only during the dwell time/beginning of sintering cycle. The transparent sample of 8YSZ was obtained at sintering temperature = 1200°C, heating/cooling rate = 2.5°C/min, dwell time = 20 min, pressure applied = 100 MPa, and point of pressure application = only during the dwell time.

The XRD analysis in **Figure 6(a)**, which shows stabilized zirconia, shows that two samples have the same chemical composition. The initial one-phase powder monoclinic (Baddeleyte) was expected, since it is at room temperature and there is no addition of stabilizer. In addition,

http://dx.doi.org/10.5772/intechopen.81323

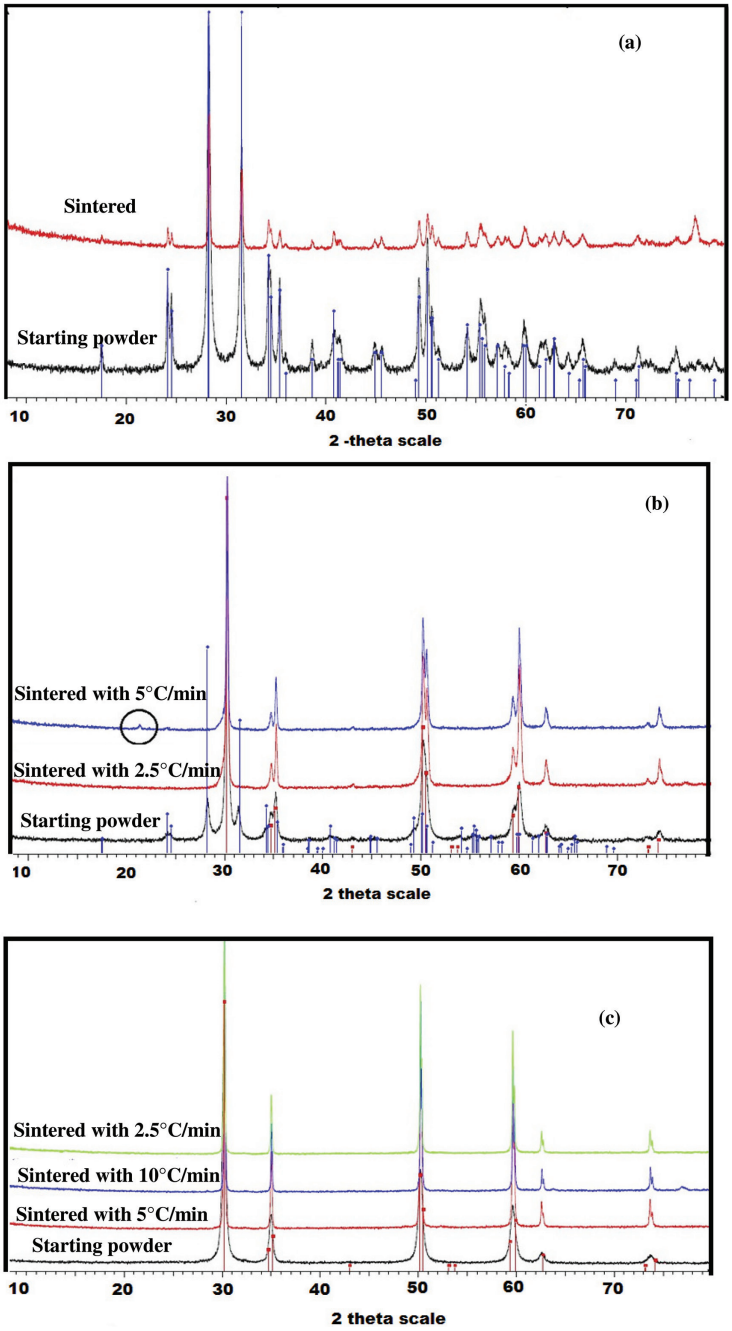

Figure 6. XRD analyses of sintered compacts of (a) pure zirconia, (b) 3YSZ, and (c) 8YSZ at 1200°C for 20 min with different heating rates.

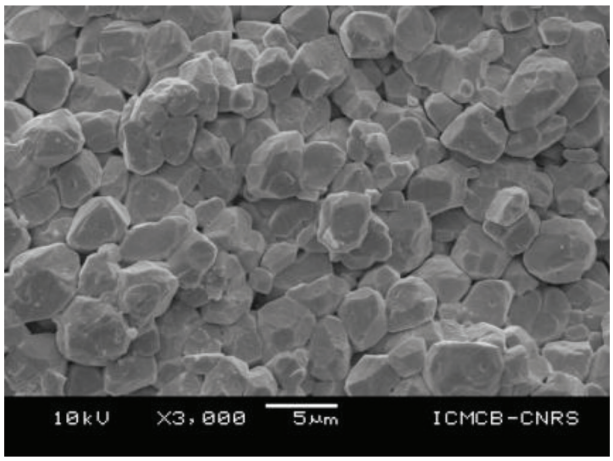

Figure 7. SEM analysis of pure zirconia at sintering temperature of 1200°C for 20 min; Heating and cooling rate: 5°C/min.

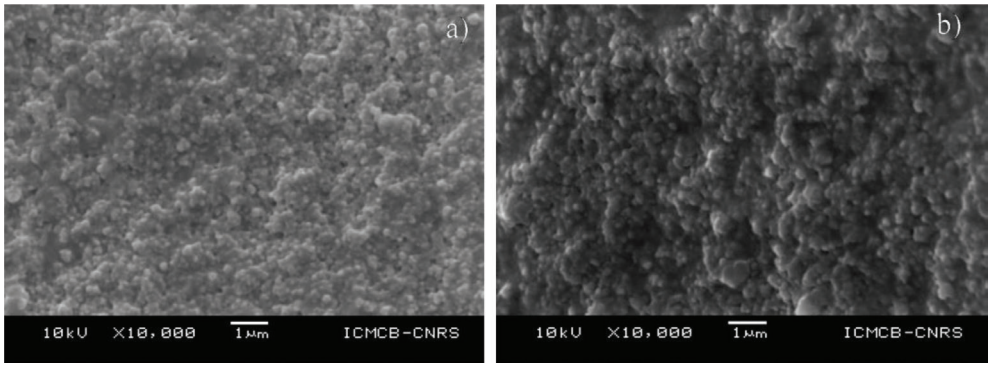

Figure 8. SEM analyses of zirconia 3YSZ at a sintering temperature of 1200°C for 20 min and at heating and cooling rates of (a) 5°C/min and (b) 10°C/min.

pure zirconia after sintering at 1200°C always has a monoclinic phase because its stabilization and sintering temperature is too low for the transition to a tetragonal phase. However, we note that the characteristic peaks of the monoclinic phase disappear more and more, which shows the beginning of a transition to a tetragonal phase. The analysis in **Figure 6(b)** shows that the three samples of 3YSZ contain the same chemical elements. The initial powder of 3YSZ has a monoclinic phase that tends to become tetragonal. For stabilized zirconia with 3% Yttria at sintering temperature of 1200° C, for heating and cooling rates 5 and 10°C/min, the tetragonal phase is obtained. However, a slight peak is observed for the 3YSZ at a heating and cooling rate of 10° C/min, which must correspond to a chemical reaction or to the fact that the corresponding heating rate is not low enough, which does not allow time for the material to change correctly of phases. The analysis in **Figure 6(c)** shows that the three samples of 8YSZ contain the same chemical elements. The initial powder of 8YSZ has a mixture of tetragonal and cubic phase that tends to become cubic. For stabilized zirconia with 8% Yttria at sintering

http://dx.doi.org/10.5772/intechopen.81323

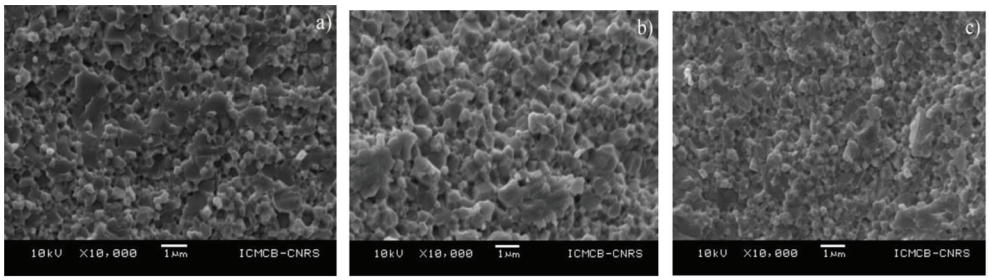

Figure 9. SEM analyzes of zirconia 8YSZ at a sintering temperature of 1200°C for 20 min and at heating and cooling rates of (a) 5°C/min; (b) 2.5°C/min; and (c) 10°C/min.

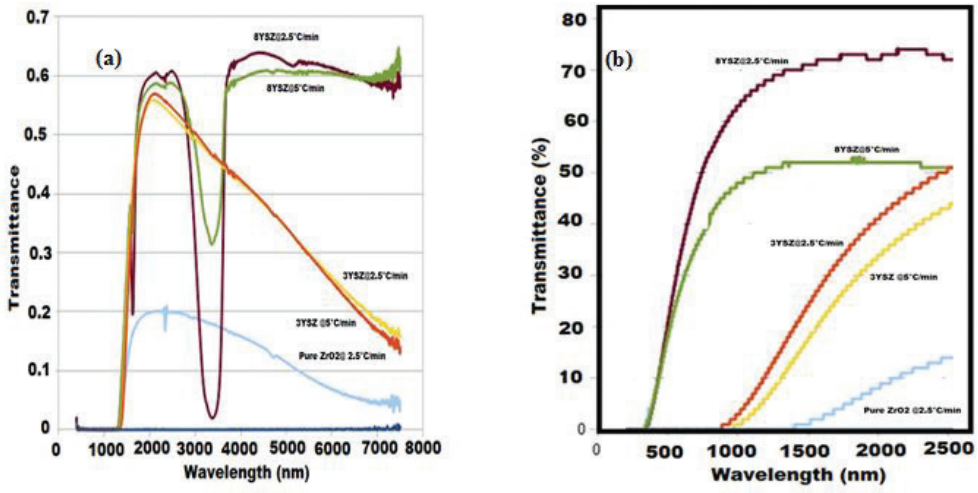

Figure 10. Transmittance spectrum of pure zirconia stabilized with yttria in (a) UV-visible range and (b) near infrared sintered at 1200°C for a dwell time of 20 min with different heating rates.

temperature of 1200°C, for heating and cooling rates of 5° and 10°C/min, the cubic phase is obtained. The conversion to the cubic phase is induced by the segregation of the Y in the grain boundaries, which were probably caused due to the slow heating rate employed during the sintering cycle (**Figures 7–9**).

The spectra of **Figure 10** show similar results. Indeed, the samples that have a maximum transmittance in the UV-visible near IR are the same as those in the IR, and the transmittance varies just slightly between the two spectra and it depends on the samples.

Zirconia stabilized with higher % yttria and the more the ceramic has high transmittance. In addition, in the case of a zirconia partially stabilized and fully stabilized, the effect of a higher or lower heating rate has a significant impact. Indeed, the lower the heating rate, the more the material has a high maximum transmittance. It is clearly evident from **Figure 10** that the transmittance corresponding to the rate of transmission is 2.5°C/min, which shows high transmittance, with transmittance of >50% in the visible and >65% in the near IR [66].

4. Conclusion

The current chapter deals with the various fabrication methodologies and syntheses of rare earth doped zirconia that can be employed for applications in areas, including catalysis, glassmaking, metallurgy, optoelectronics, batteries, and coatings for extreme environments. During recent years, it has been reported that using mixed rare earth oxides as dopant may strongly improve the functional properties of the matrix such as increasing thermal shock resistance of zirconia-based thermal barrier coatings (TBCs) and improve ionic conductivity of solid oxide fuel cells (SOFCs) by surface segregation mechanisms. Various powder syntheses methodologies with an accent on hydrothermal powder synthesis is discussed. The feasibility of obtaining the sintering compacts of rare earth oxides and co-doped rare earth oxides both from the commercial and hydrothermal syntheses by rapid sintering methods such as spark plasma sintering is demonstrated. The role of rare earth oxides on sintering and in the point of view of applications is evident from the current work for the zirconia. Further investigations are necessary to validate the role of co-doped rare earth oxides for thermal barrier coatings and in SOFCs. The aforesaid is being investigated as a part of the project "MONAMIX" and will be reported elsewhere later.

Acknowledgements

The authors duly acknowledge the following funding agencies for the present work through

1. Grant agreement 692216 SUPERMAT from European Union's Horizon 2020 research and innovation program
2. Grant agreement ERAMIN 2 COFUND-Research & Innovation program on raw materials to foster circular economy-"MONAMIX"- "ANR-17-MIN2-0003-03"
3. Part of collaboration in photonics between University of Bordeaux and Huazhong University of Science and Technology.

Author details

Mythili Prakasam[1]*, Sorina Valsan[3], Yiying Lu[1,2], Felix Balima[1], Wenzhong Lu[2], Radu Piticescu[3] and Alain Largeteau[1]

*Address all correspondence to: mythili.prakasam@icmcb.cnrs.fr

1 CNRS, University of Bordeaux, ICMCB, UMR 5026, Pessac, France

2 Huazhong University of Science and Technology (HUST) School of Optical and Electronic Information, Wuhan, China

3 National R&D Institute for Nonferrous and Rare Metals, Pantelimon, Romania

References

[1] Bangchao Y, Jiawen J, Yican Z. Spark-plasma sintering the 8-mol% yttria-stabilized zirconia electrolyte. Journal of Materials Science. 2004;**39**:6863-6865

[2] Takeuchi T, Kondoh I, Tamari N, Balakrishnan N, Nomura K, Kageyama H, et al. Improvement of mechanical strength of 8 mol% yttria-stabilized zirconia ceramics by spark-plasma sintering. Journal of the Electrochemical Society. 2002;**149**:A455-A461

[3] Cao XQ, Vassen R, Stoever D. Ceramic materials for thermal barrier coatings. Journal of the European Ceramic Society. 2004;**24**:1-10

[4] Rambo CR, Cao J, Sieber H. Preparation, and properties of highly porous, biomorphic YSZ ceramics. Materials Chemistry and Physics. 2004;**87**:345-352

[5] Balakrishnan N, Takeuchi T, Nomura K, Kageyama H, Takeda Y. Aging effect of 8 mol% YSZ ceramics with different microstructures. Journal of the Electrochemical Society. 2004;**151**:A1286-A1291

[6] Li Q, Zhang YF, Ma XF, Meng J, Cao XQ. High-pressure sintered yttria stabilized zirconia ceramics. Ceramics International. 2009;**35**:453-456

[7] Patil DS, Prabhakaran K, Durgaprasad C, Gokhale NM, Samui AB, Sharma SC. Synthesis of nanocrystalline 8 mol% yttria stabilized zirconia by the oleate complex route. Ceramics International. 2009;**35**:515-519

[8] Rajeswari K, Padhi S, Reddy ARS, Johnson R, Das D. Studies on sintering kinetics and correlation with the sinterability of 8Y zirconia ceramics based on the dilatometric shrinkage curves. Ceramics International. 2013;**39**:4985-4990

[9] Kubrin R, do Rosario JJ, Lee HS, Mohanty S, Subrahmanyam RP, Smirnova I, et al. Vertical convective coassembly of refractory YSZ inverse opals from crystalline nanoparticles. ACS Applied Materials & Interfaces. 2013;**5**:13146-13152

[10] Miura N, Jin H, Wama R, Nakakubo S, Elumalai P, Plashnitsa V. Novel solid-state manganese oxide-based reference electrode for YSZ-based oxygen sensors. Sensors and Actuators B: Chemical. 2011;**152**:261-266

[11] Garbayo I, Tarancón A, Santiso J, Peiró J, Alarcón-LLadó E, Cavallaro A, et al. Electrical characterization of thermomechanically stable YSZ membranes for micro solid oxide fuel cells applications. Solid State Ionics. 2010;**181**:322-331

[12] Drescher I, Lehnert W, Meusinger J. Structural properties of SOFC anodes and reactivity. Electrochimica Acta. 1998;**43**:3059-3068

[13] Inuzuka M, Nakamura S, Kishi S, Yoshida K, Hashimoto K, Toda Y, et al. Effect of hydroxyapatite dopant to yttria stabilized zirconia ceramics for biomedical application. Phosphorus Research Bulletin. 2003;**16**:75-82

[14] Klimke J, Trunec M, Krell A. Transparent tetragonal yttria-stabilized zirconia ceramics: Influence of scattering caused by birefringence. Journal of the American Ceramic Society. 2011;**94**:1850-1858

[15] Chevalier J, Gremillard L, Virkar AV, Clarke DR. The tetragonal-monoclinic transformation in zirconia: Lessons learned and future trends. Journal of the American Ceramic Society. 2009;**92**:1901-1920

[16] Bokhimi X, Morales A, García-Ruiz A, Xiao TD, Chen H, Strutt PR. Transformation of yttrium-doped hydrated zirconium into tetragonal and cubic nanocrystalline zirconia. Journal of Solid State Chemistry. 1999;**142**:409-418

[17] Yashima M, Hirose T, Kakihana M, Suzuki Y, Yoshimura M. Size and charge effects of dopant M on the unit-cell parameters of monoclinic zirconia solid solutions $Zr_{0.98}M_{0.02}O_2$–δ (M = Ce, La, Nd, Sm, Y, Er, Yb, Sc, Mg, Ca). Journal of the American Ceramic Society. 1997;**80**:171-175

[18] Suárez G, Garrido LB, Aglietti EF. Sintering kinetics of 8Y–cubic zirconia: Cation diffusion coefficient. Materials Chemistry and Physics. 2008;**110**:370-375

[19] Yamashita I, Tsukuma K. Light scattering by residual pores in transparent zirconia ceramics, Lattice diffusion kinetics in Y_2O_3-stabilized cubic ZrO_2 single crystals: A dislocation loop annealing study. Journal of the Ceramic Society of Japan. 2011;**119**:133-135

[20] Chien FR, Heuer AH. Lattice diffusion kinetics in Y_2O_3-stabilized cubic ZrO_2 single crystals: A dislocation loop annealing study. Philosophical Magazine A. 1996;**73**:681-697

[21] Lu J, Ueda K-i, Yagi H, Yanagitani T, Akiyama Y, Kaminskii AA. Neodymium doped yttrium aluminum garnet ($Y_3Al_5O_{12}$) nanocrystalline ceramics—a new generation of solid state laser and optical materials. Journal of Alloys and Compounds. 2002;**341**:220-225

[22] Pampuch R, Haberko K. In: Vincezini P, editor. Ceramic Powders. Elsevier Publ. Co.; 1983. pp. 623-634

[23] Gope W, Reinhardt G, Rosch M. Trends in the development of solid state amperometric and potentiometric high temperature sensors. Solid State Ionics. 2000;**136**:519-531

[24] Ciachi FT, Badwal SP. The system Y_2O_3–Sc_2O_3–ZrO_2: Phase stability and ionic conductivity studies. Journal of the European Ceramic Society. 1991;**7**:197-206

[25] Menil F, Coillard V, Debeda H, Lucat C. A simplified model for the evaluation of the electrical resistance of a zirconia substrate with co-planar electrodes. Sensors and Actuators. 2001;**B77**:84-89

[26] Piticescu RR, Monty C, Millers D. Hydrothermal synthesis of nanostructured materials: Present state and future prospects. Sensors and Actuators B. 2005;**109**:102-106

[27] Kosacki I, Colomban P, Anderson HV. Proceedings of the US–Japan Workshop on Electrically Active Ceramic Interfaces. MIT, USA; 1998. pp. 180-188

[28] Wepner W. Tetragonal zirconia polycrystals-a high performance solid oxygen ion conductor. Solid State Ionics. 1992;**52**:15-21

[29] Mahato N, Banerjee A, Gupta A, Omar S, Balani K. Progress in material selection for solid oxide fuel cell technology: A review. Progress in Materials Science. 2015;**72**:141-337

[30] Manjunatha S, Hari Krishna R, Thomas T, Panigrahi BS, Dharmaprakash MS. Moss-Burstein effect in stable, cubic ZrO_2:Eu^{+3} nanophosphors derived from rapid microwave-assisted solution-combustion technique. Materials Research Bulletin. 2018;**98**:139-147

[31] Lovisa LX, Araújo VD, Tranquilin RL, Longo E, Li MS, Paskocimas CA, et al. White photoluminescence emission from ZrO_2 co-doped with Eu^{3+}, Tb^{3+} and Tm^{3+}. Journal of Alloys and Compounds. 2016;**674**:245-251

[32] Hui Y, Zou B, Liu S, Zhao S, Xu J, Zhao Y, et al. Effects of Eu^{3+}-doping and annealing on structure and fluorescence of zirconia phosphors. Ceramics International. 2015; **41**:2760-2769

[33] Guerra AIR, Merlín IM, Falcony C. The role of the stabilizing agent on the structural and luminescent properties of hydrothermally synthesized ZrO_2:Tb^{3+} phosphors. Ceramics International. 2018;**44**:13744-13749

[34] Hongmin AO, Xiangsheng L, He Z, Jing Z, Xiaowei H, Zongyu F, et al. Preparation of scandia stabilized zirconia powder using microwave-hydrothermal method. Journal of Rare Earths. 2015;**33**:746-751

[35] Mekala R, Deepa B, Rajendran V. Preparation, characterization and antibacterial property of rare earth (Dy and Ce) doping on ZrO_2 nanoparticles prepared by co-precipitation method. Materials Today: Proceedings. 2018;**5**:8837-8843

[36] Kumar V, Balasubramanian K. Progress update on failure mechanisms of advanced thermal barrier coatings: A review. Progress in Organic Coatings. 2016;**90**:54-82

[37] Quarles G. Comparison of Optical, Mechanical and Thermo-Optical Properties of Oxide Polycrystalline Laser Gain Materials with Single Crystals. USA: Optical Society of America; 2006

[38] Hu C. Developments in hot pressing (HP) and hot isostatic pressing (HIP) of ceramic matrix composites. In: Advances in Ceramic Matrix Composites. 2014. pp. 164-189

[39] Huo D, Zheng Y, Sun X, Li X, Liu S. Preparation of transparent Y_2O_3 ceramic by slip casting and vacuum sintering. Journal of Rare Earths. 2012;**30**:57-62

[40] Reddy VR, Upadhyay SK, Gupta A, Awasthi AM, Hussain S. Enhanced dielectric and ferroelectric properties of $BaTiO_3$ ceramics prepared by microwave assisted radiant hybrid sintering. Ceramics International. 2014;**40**:8333-8339

[41] Fu P, Lu W, Lei W, Xu Y, Wang X, Wu J. Transparent polycrystalline $MgAl_2O_4$ ceramic fabricated by spark plasma sintering: Microwave dielectric and optical properties. Ceramics International. 2013;**39**:2481-2487

[42] Bangi UKH, Park C-S, Baek S, Park H-H. Sol-gel synthesis of high surface area nanostructured zirconia powder by surface chemical modification. Powder Technology. 2013; **239**:314-318

[43] Díaz-Parralejo A, Macías-García A, Sánchez-González J, Ángeles Díaz-Díez M, Eduardo M. Cuerda-Correa; a novel strategy for the preparation of yttria-stabilized zirconia

powders-deposition and scratching of thin films obtained by the sol-gel method. Journal of Non-Crystalline Solids. 2011;**357**:1090-1095

[44] Yao W, Tang Z, Zhang Z, Luo S. Preparation of 8 mol% yttria-stabilized zirconia by an oil flotation-assisted chemical coprecipitation route. Materials Letters. 2002;**57**:502-506

[45] Yuan FL, Chen CH, Kelder EM, Schoonman J. Preparation of zirconia and yttria stabilized zirconia (YSZ) fine powders by flame assisted ultrasonic spray pyrolysis. Solid State Ionics. 1998;**109**:119-123

[46] Gaudon M, Djurado E, Menzler NH. Morphology and sintering behaviour of yttria stabilised zirconium (8-YSZ) powders synthesized by spray pyrolysis. Ceramics International. 2004;**30**:2295-2303

[47] Somiya S, Akiba T. Hydrothermal zirconia powders: A Bibliography. Journal of the European Ceramic Society. 1999;**19**:81-87

[48] Oliveira AP, Torem ML. The influence of precipitation variables on zirconia powder synthesis. Powder Technology. 2001;**119**:181-193

[49] Byrappa K, Yoshimura M. Handbook of Hydrothermal Technology. 2nd ed. Elsevier Inc; 2012

[50] Piticescu RR, Hrovath M, Belavic D, Ionascu A, Malic B, Motoc AM, et al. Zirconia pressure sensors: From nanopowders to device. In: Solid State Phenomena. Vol. 99. Switzerland: Transtech Publications; 2004. pp. 89-98

[51] Wei Chen I, Wang WH. Sintering dense nanocrystalline ceramics without final-stage grain growth. Nature. 2000;**404**:168-171

[52] Charles Greskovich D, William Minnear P, Milivoj Brun K, Robert Riedner J. Preparation of high uniformity polycrystalline ceramics by presintering, hot isostatic pressing and sintering and the resulting ceramic. US5013696 A; 1991

[53] Omori M. Sintering, consolidation, reaction, and crystal growth by the spark plasma system (SPS). Materials Science and Engineering A. 2000;**287**:183-188

[54] Agrawal DK. Microwave processing of ceramics. Current Opinion in Solid State and Materials Science. 1998;**3**:480-485

[55] Alaniz JE, Perez-Gutierrez FG, Aguilar G, Garay JE. Optical properties of transparent nanocrystalline yttria stabilized zirconia. Optical Materials. 2009;**32**:62-68

[56] Kim M-J, Ahn J-S, Kim J-H, Kim H-Y, Kim W-C. Effects of the sintering conditions of dental zirconia ceramics on the grain size and translucency. The Journal of Advanced Prosthodontics. 2013;**5**:161-166

[57] Jiang L, Liao Y, Wan Q, Li W. Effects of sintering temperature and particle size on the translucency of zirconium dioxide dental ceramic. Journal of Materials Science: Materials in Medicine. 2011;**22**:2429-2435

[58] Yi F, Cheng J, Roy R, Roy DM, Agrawal DK. Enhancing densification of zirconia-containing ceramic-matrix composites by microwave processing. Journal of Materials Science. 1997;**32**:4925-4930

[59] Anselmi-Tamburini U, Woolman JN, Munir ZA. Transparent nanometric cubic and tetragonal zirconia obtained by high-pressure pulsed electric current sintering. Advanced Functional Materials. 2007;**7**:3267-3273

[60] Casolco SR, Xu J, Garay JE. Transparent/translucent polycrystalline nanostructured yttria stabilized zirconia with varying colors. Scripta Materialia. 2008;**58**:516-519

[61] Krell A, Hutzler T, Klimke J. Defect strategies for an improved optical quality of transparent ceramics. Optical Materials. 2014;**38**:61-74

[62] Yamashita I, Kudo M, Tsukuma K. Development of highly transparent zirconia ceramics. TOSOH Research & Technology Review. 2012;**56**:11-16

[63] Miao X, Sun D, Hoo PW, Liu J, Hu Y, Chen Y. Effect of titania addition on yttria-stabilised tetragonal zirconia ceramics sintered at high temperatures. Ceramics International. 2004; **30**:1041-1047

[64] Dragut DV, Badilita V, Motoc AM, Piticescu RR, Zhao J, Hijji H, et al. Thermal stability and field assisted sintering of cerium-doped YSZ ceramic nanoparticles obtained via a hydrothermal process. Manufacturing Review. 2017;**4**(11):18-28

[65] Cho J, Weng H, Fan Z, Xue S, Vikrant KSN, Wang H, et al. High temperature deformability of ductile flash-sintered ceramics via in-situ compression. Nature Communications. 2018;**9**:2063-2068

[66] Prakasam M, Weill F, Lebraud E, Viraphong O, Buffiére S, Largeteau A. Densification of 8Y-tetragonal-stabilized zirconia optoceramics with improved optical properties by Y segregation. International Journal of Applied Ceramic Technology. 2016;**2016**(13):904-911